

**IDENTIFICATION OF HIGHLY SILICIC FEATURES ON THE MOON.** T. D. Glotch<sup>1</sup>, P. G. Lucey<sup>2</sup>, J. L. Bandfield<sup>3</sup>, B. T. Greenhagen<sup>4</sup>, I. R. Thomas<sup>5</sup>, R. C. Elphic<sup>6</sup>, N. E. Bowles<sup>5</sup>, M. B. Wyatt<sup>7</sup>, C. C. Allen<sup>8</sup>, K. L. Donaldson-Hanna<sup>7</sup>, and D. A. Paige<sup>9</sup>. <sup>1</sup>Stony Brook University, <sup>2</sup>HIGP, University of Hawaii, <sup>3</sup>University of Washington, <sup>4</sup>Jet Propulsion Laboratory, <sup>5</sup>Oxford University, <sup>6</sup>NASA Ames, <sup>7</sup>Brown University, <sup>8</sup>NASA JSC, <sup>9</sup>University of California, Los Angeles.

**Introduction:** The Diviner Lunar Radiometer Experiment (Diviner) is a multispectral radiometer that is well-suited to detecting the mineral indicators of silicic magmatism. Diviner has three narrow spectral band-pass filters centered at 7.8, 8.25, and 8.55  $\mu\text{m}$  (channels 3-5). These three “8  $\mu\text{m}$ ” channels were specifically designed to characterize the position of the silicate Christiansen Feature (CF) [1], which is directly sensitive to silicate mineralogy and bulk  $\text{SiO}_2$  content of a material [2]. We have used Diviner data to identify the most silicic regions on the Moon. These include Hansteen Alpha, the Lassell Massif, the Gruithuisen Domes, and Aristarchus crater. Each of these regions is located within the Procellarum Kreep Terrane (PKT) defined by [3] and is correlated both with well-known “red spots” and high Th anomalies in Lunar Prospector GRS data [4-7]. Previously defined red spots, including Helmet and southern Montes Rhiphaeus, that do not exhibit Th anomalies do not appear to be anomalously silicic in Diviner data.

**Methods:** Using Diviner data acquired between Sept. and Nov. 2009, we compared the mid-IR spectral shapes of several lunar red spots to surrounding mare and highlands materials, regions known to be pure plagioclase feldspar, and laboratory emissivity spectra of minerals and analogs. For our analyses, we selected data acquired near noon, with low ( $<8^\circ$ ) emission angles, and surface temperatures  $>320$  K. We geometrically binned data from each of the seven spectral bands at 32 pixels per degree ( $\sim 950$  m/pixel at the equator). Radiance data were converted to equivalent emissivity by dividing the radiance at each channel by the radiance of a blackbody at the highest brightness temperature measured between Diviner’s 8  $\mu\text{m}$  channels.

We defined two spectral indices to map the spectral variability in Diviner data. The first spectral index measures the slope between channels 3 and 4 in the form  $I = \epsilon_3 - \epsilon_4$ , where  $\epsilon_3$  and  $\epsilon_4$  are the emissivities in channels 3 and 4 respectively (centered near 7.8 and 8.25  $\mu\text{m}$ ). A second spectral index,  $c$ , determines the direction of concavity between channels 3-5 (centered near 7.8 and 8.55  $\mu\text{m}$ ). Briefly, we define a line using channels 3 and 5 and interpolate the value of the channel 4 emissivity on this line. We then subtract the true channel 4 emissivity from this value. A positive value of this index is indicative of a concave up shape, while a negative index value is indicative of a concave down

shape. Mafic materials have negative slope and concavity index values, while more intermediate materials have positive slope index values. Only the most silicic materials such as quartz, high-Si glass, and some sodic/potassic feldspars have positive values of both the slope and concavity indices (Fig. 1) due to the fact that their CFs occur at wavelengths well shortward of the Diviner 8  $\mu\text{m}$  channels.

**Results:** The concave upward shapes and positive slope indices in the spectra of Hansteen Alpha, Lassell Massif, the Gruithuisen Domes, and the southern rim and ejecta of Aristarchus crater, indicate the presence of highly silicic evolved lithologies (Figs 2-3). The implied evolved compositions are consistent with strong positive anomalies of Th, an incompatible large ion lithophile element [8]. Red spots that lack correlated high Th anomalies, including Helmet and southern Montes Rhiphaeus (Fig. 2e) also lack the unique concave-up spectral character in Diviner data, confirming a lack of silicic indicator minerals (Fig 3).

Diviner spectra of each of the silicic red spots are also distinct from those of the surrounding terrains. Both mare and highlands materials in each region have spectral shapes with negative concavity and slope index values (Fig 3). The previously known most silicic regions on the Moon are the areas composed of nearly pure anorthite based on VNIR spectral observations [9-10]. Diviner spectra of pure plagioclase from the inner ring of the Orientale multiring impact basin (Figure 4) are concave down with a negative slope index. Of all the feldspars, anorthite has the longest CF position, and this comparison indicates that the red spots with CF positions shorter than the areas of pure anorthite, along with positive slope and concavity indices are composed of quartz, or Si-rich glass, perhaps mixed with Na- or K-rich feldspars.

**Discussion and Conclusions:** The Gruithuisen domes and Hansteen Alpha have previously been proposed to be silicic volcanic constructs [7, 11]. Diviner data support interpretations of these features as non-mare volcanic domes analogous to terrestrial rhyolite domes. By contrast, the Aristarchus and Lassell regions appear to be sampling silicic lithologies emplaced at depth. In both cases, the Diviner spectra consistent with silicic compositions are confined to craters and their ejecta.

Both silicate liquid immiscibility (SLI) and basaltic underplating have been proposed as mechanisms to

create highly silicic magmas on the moon [7,12]. SLI is not likely to be responsible for large extrusive volcanic constructs such as Hansteen Alpha and the Gruithuisen domes, because this process requires nearly complete fractional crystallization before relatively small volumes of silicic magmas are formed. Basaltic underplating is a likely mechanism for the formation of these features. It is possible, however, that large granitic plutons could have been produced within the lunar crust as a result of the slow crystallization of late-stage magma ocean residual melt [13-14]. This slow-cooling method would preclude the formation of large volumes of extrusive lavas [7], but it is a reasonable scenario for the formation of large granitic bodies that could be exposed by impact craters, as in the case of Aristarchus and Lassell.

We are currently searching the Diviner data set for other examples of extreme lithologies, including additional silicic regions as well as highly mafic compositions [15]. The Diviner data set is complementary to existing VNIR and chemical data sets and will be useful in placing additional constraints on the composition of the lunar crust.

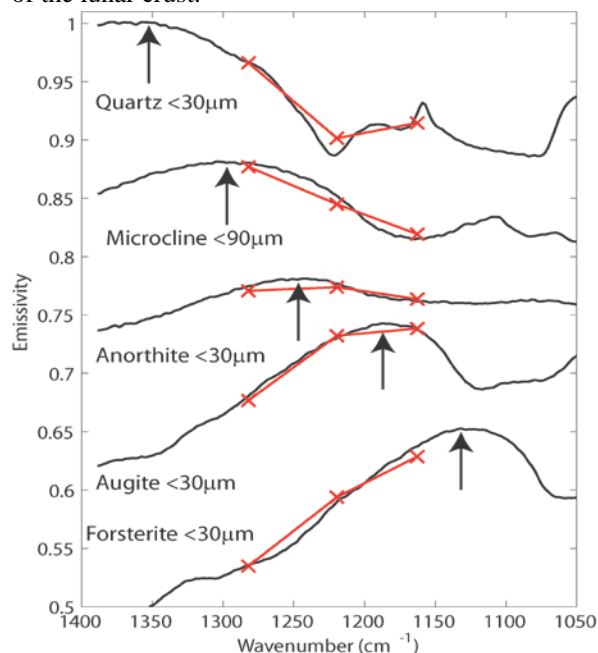


Figure 1. Full resolution laboratory spectra acquired under ambient conditions (black) and those same spectra convolved to the Diviner 8  $\mu\text{m}$  channel spectral bandpasses. Only the most silicic materials display a concave-up spectral shape. Arrows mark the CF positions for each mineral. We are currently acquiring mineral spectra in a simulated lunar environment. [16].

**References:** [1] Greenhagen B. T. (2009) *Ph.D. Thesis, UCLA*. [2] Logan L. M. et al. (1973) *J. Geophys. Res.*, 78, 4983-5003. [3] Jolliff B. L. et al. (2000) *J. Geophys. Res.*, 105(E2), 4197-4216. [4] Wood C. A. and J. W. Head (1975)

*Conf. Origin Mare Basalts*. [5] Bruno B. C. et al. (1991) *LPS XXI*, 405-415. [6] Hagerty J. J. et al. (2006) *J. Geophys. Res.*, 111(E6), doi:10.1029/2005JE002592 [7] Chevrel S. D. et al. (1999) *J. Geophys. Res.*, 104(E7), 16515-16529. [8] Hagerty J. J. et al. (2009) *J. Geophys. Res.*, 114(E4), doi:10.1029/2008JE003262. [9] Spudis P. D. et al. (1984) *J. Geophys. Res.*, 89, C197-C210. [10] Ohtake M. et al. (2009) *Nature*, 461, 236-241. [11] Hawke B. R. et al. (2003) *J. Geophys. Res.*, 108(E7), doi:10.1029/2002JE002013. [12] Jolliff B. L. et al. (1999) *Am. Miner.* 84, 821-837. [13] Neal C. R. and L. A. Taylor (1989) *Geochim. Cosmochim. Acta*, 53, 529-541. [14] Jolliff B. L. (1998) *Int. Geol. Rev.*, 40, 916-935. [15] Greenhagen B. T. et al. (2010) *LPS XXI*. [16] Thomas I. R. et al. (2010) *LPS XXI*.

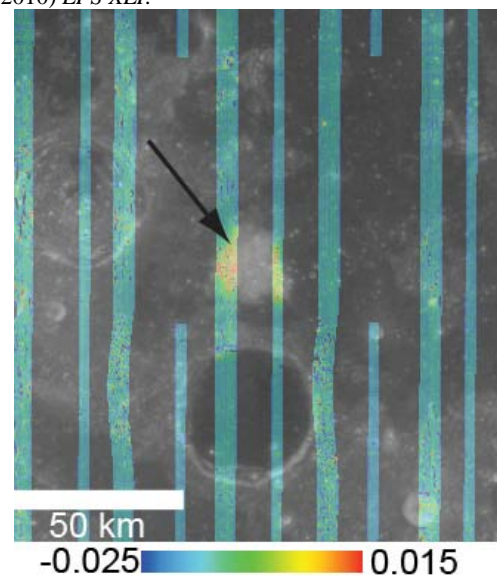


Figure 2. Diviner concavity index map of Hansteen Alpha overlain on a Clementine 750 nm mosaic. Index values range from -0.025 to 0.015.

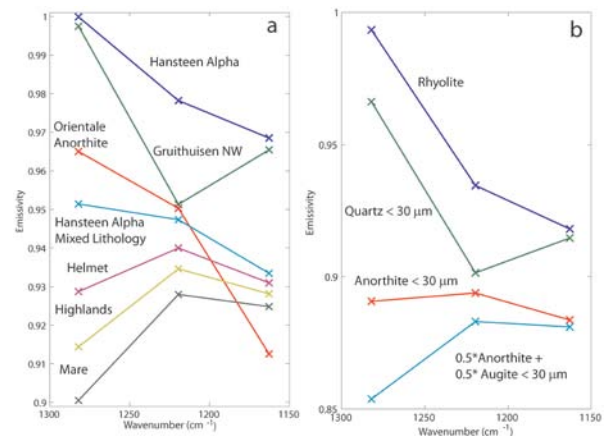


Figure 3. a) Diviner spectra from several silicic red spots, Orientale pure plagioclase, and more typical lunar materials. b) Laboratory spectra convolved to Diviner Bandpasses